

SENSITIVITY OF OZONE CONCENTRATIONS TO VOC AND NO_x EMISSIONS IN THE CANADIAN LOWER FRASER VALLEY

WEIMIN JIANG, DONALD L. SINGLETON, MARK HEDLEY and ROBERT McLAREN*

Institute for Chemical Process and Environmental Technology, National Research Council Canada, Ottawa, Ont., Canada K1A 0R6

Abstract—The SAPRC90 chemical mechanism module implemented in CALGRID is updated for the specific emissions and applications of the Lower Fraser Valley (LFV) of British Columbia, Canada. The kinetic and mechanistic parameters of lumped VOC reactions recalculated using the LFV emissions profiles are noticeably different from those based on default emissions profiles, indicating the importance of tailoring the parameters to specific regions. The sensitivities of ozone concentrations to total and speciated VOC and NO_x emissions as well as to the NO₂/NO_x ratios are determined. Significant VOC model species are identified based on the impact of their emissions on ozone formation in the LFV. Of note is the importance of the emissions of a lumped class of aromatics, ARO2, which contains mostly isomers of xylene and trimethylbenzene and is derived chiefly from the use and distribution of gasoline fuels. The ARO2 emissions make the largest contribution of all model VOC species to the ozone levels in the urban plume. The results indicate that reduction of ARO2 emissions alone could achieve significant reduction of ozone levels in the LFV. Base case emissions of NO_x (NO or NO₂) in the LFV contribute negatively to the ozone formation. Any overestimation of NO_x or underestimation of VOC in the emissions inventory could cause underestimations of ozone levels by photochemical models. Crown copyright © 1996 Published by Elsevier Science Ltd

Key word index: Photochemical modelling, air pollution, smog, emissions, sensitivity.

I. INTRODUCTION

Elevation of ground-level ozone has been a serious concern in the past several decades. Despite all the research and control measures during this period, there is still no convincing evidence that the problem is completely under control (NRC, 1991). To understand the complicated process of ozone formation, trajectory models and three-dimensional grid models are widely used to calculate ozone levels based on emissions inventories, chemistry and meteorology. However, models often underpredict ozone levels. Deficiencies in emissions inventories are frequently cited as the reasons for the underprediction although there are other potential causes, including deficiencies in the chemical mechanisms.

In this paper, we study the sensitivity of ozone concentrations to VOC and NO_x emissions in the Lower Fraser Valley (LFV) region near Vancouver, British Columbia, and the Canada–U.S. border. The region has been identified as one of the three ozone

non-attainment areas in Canada by the Management Plan for Nitrogen Oxides (NO_x) and Volatile Organic Compounds (VOCs) (CCME, 1990). Ozone concentrations in the region during summer episodes frequently exceed the 82 ppb maximum acceptable level in Canada. Similar to many other modelling efforts conducted in other regions of North America, our initial modelling results in the LFV consistently underpredicted daytime maximum ozone concentrations. Although it is widely believed that the reason for the underprediction of ozone is an underestimation of VOC emissions, further studies are needed to support this understanding. Instead of just categorically citing total underestimated VOC emissions as the cause of underpredicting ozone, it is also necessary to study the impact of speciated NO_x and VOC emissions on the ozone concentrations.

The results shown in this paper present the sensitivity of ozone concentrations to both total VOC and NO_x emissions as well as to the speciated emissions in the LFV. We also present the effects of the NO₂/NO_x ratio on the ozone concentrations. For its computational efficiency, the OZIPR trajectory model (Gery and Crouse, 1989) is chosen in this study. The chemical mechanism used in our 3-D CALGRID model

*Current address: Department of Chemistry and Centre for Atmospheric Chemistry, York University, North York, Ontario, Canada M3J 1P3.

(Yamartino *et al.*, 1992) is incorporated into the OZIPR model to ensure the consistency in chemistry. Some kinetic and mechanistic parameters in the chemical mechanism, which is a modified and lumped version of the SARPC90 mechanism (Carter, 1990), are updated to reflect the emissions characteristics of the LFV. A moderate ozone episode which occurred 17–21 July 1985 was selected to conduct the study. The gridded LFV emissions inventory, prepared for CALGRID for the ozone episode, is reprocessed to produce hourly speciated emissions along a selected trajectory for an urban plume. The emissions inventory was originally developed based upon the Lower Mainland Emissions Inventory in Canada and an inventory of sources in Whatcom County in the U.S. (McLaren *et al.*, 1995). A regional forecast model, MC2 (Tanguay *et al.*, 1990) is used to calculate meteorological conditions for this study.

2. METHODOLOGY

2.1. The OZIPR model and the CD2243V2 mechanism

OZIPR is a research-oriented version of EPA's OZIPP (Ozone Isopleth Plotting Package) computer modelling program. It has enhanced input–output capability compared to OZIPP. Structure of the program is similar to that of the OZIPM-4 model, which is documented by Hogo and Gery (1988). As a trajectory model, OZIPR simulates complex chemical and physical processes of an air column moving along the wind trajectory in the mixed layer. Emissions are injected into the air column hourly. Air above the column is

mixed in as the mixing height rises during the day and causes entrainment dilution if the aloft air is cleaner than the air in the mixed layer. Various chemical mechanisms can be selected and incorporated into the model using the specified format. Dry depositions of model species are treated as an option, and they are not included in this paper because the big uncertainties in the deposition rates could affect the focus of this paper on emissions sensitivity.

The chemical mechanism used in a recent version of the CALGRID 3-D model (version 1.5/S90, level 921130) is processed into the OZIPR format. The mechanism is integrated with the OZIPR model to ensure the consistency in chemistry between the two models used in our research. The mechanism, named COND2243, is a modified and lumped version of the SAPRC 90 mechanism (Carter, 1990). It contains 54 chemical species and 129 reactions. Among the 54 chemical species, there are two lumped alkanes, two lumped aromatics and three lumped olefins. The chemistry of methanol (MEOH), ethanol (ETOH), methyl *t*-butyl ether (MTBE) and methane (CH_4) is treated explicitly. The explicit treatment of these species is needed for our studies on impacts of alternative fuels and reformulated gasolines on air quality. Among the 129 chemical reactions, 16 are reactions of lumped VOC model species with OH, O_3 , $\text{O}(^3\text{P})$ and NO_3 .

Kinetic and mechanistic parameters of lumped VOC species and their reactions in the COND2243 mechanism are updated to reflect the emissions characteristics of the LFV modelling region, shown in Fig. 1. Anthropogenic emissions, including mobile, point and area source emissions, are concentrated in Vancouver and surrounding urban areas. Biogenic sources have significant contributions to the total emissions in part because of the large forest areas in the mountains. Total VOC emissions in the LFV modelling domain on 19 July 1985, which is a typical ozone episode day, are used to build an average VOC emissions profile. The profile contains mass emissions of each of the 574 emitted VOC classes during the day. Rate constants and product

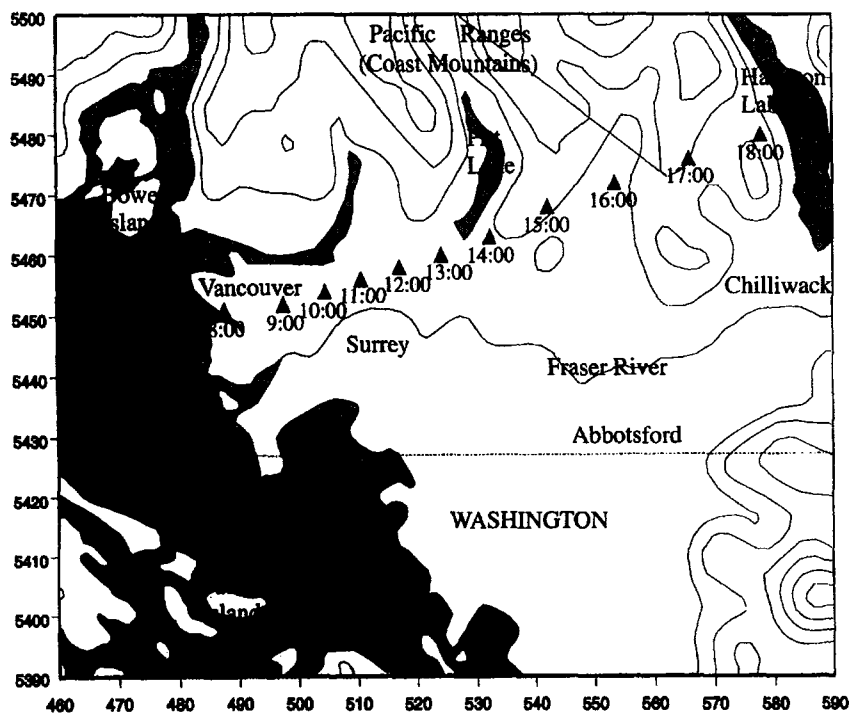


Fig. 1. The Lower Fraser Valley (LFV) modelling region. The selected air mass trajectory for the period 6:00–18:00, 18 July 1985 is shown by a series of black triangles. Numbers on the horizontal and vertical axis are UTM (Universal Transverse Mercator) coordinates in km (in UTM zone 10).

yields of lumped VOC reactions as well as carbon numbers of lumped VOC model species are recalculated based on this profile. The updated mechanism that matches the LFV emissions profile is named CD2243V2 to indicate that it is the modified version 2 of the COND2243 mechanism using the Vancouver area's emissions inventory.

In the CD2243V2 mechanism, 574 emitted VOC classes are represented by 18 model species, which are the same as the model species in the COND2243 mechanism. Table 1 lists the model species names and their descriptions. The non-methane-organic compound (NMOC) emissions profile, represented as model species, is shown in Fig. 2. Model species ALK1 and OLE3 make the biggest contribution to the NMOC emissions. For OLE3, the majority of the emissions are from biogenic sources. Methane, which is not included in Fig. 2, is about 46% of the total emissions of organic gases on a carbon basis.

The LFV emissions profile is different from the default emissions profile used in calculating the relevant parameters for the COND2243 mechanism in CALGRID. The difference in relative amount of emitted VOC classes in the emissions profiles results in the change in the calculated parameters for lumped VOC reactions and lumped VOC species. Although it is tedious to compare the differences between the two emitted VOC mixtures, which contain 295 and 574 emitted VOC classes, respectively, Table 2 shows

rate constant and carbon number changes caused by these differences. For example, the rate constants for the reactions $\text{OLE1} + \text{NO}_3$ and $\text{OLE3} + \text{NO}_3$ change by 77 and 75% on going to the CD2243V2 mechanism. The carbon number of the lumped model species OLE3 increases 31% from 6.53 in the COND2243 mechanism to 8.55 in the CD2243V2 mechanism for the LFV. The changes reflect more isobutene emissions in the OLE1 group and a larger contribution of emitted monoterpenes to OLE3 in the LFV. Similar changes also occurred for mechanistic parameters.

To facilitate the process of chemical mechanism conversion, parameter calculation, and emissions processing, Carter's mechanism preparation software package (Carter, 1988) and U.S. EPA's Emissions Processing System 2 (EPS2) (Gardner *et al.*, 1992) are integrated into our modelling system and used in this study.

2.2 Input to the OZIPR trajectory model

The input to the OZIPR model includes initial concentrations in the mixed and aloft layers and hourly emissions, mixing heights, temperature and relative humidities. For 18 July 1985, a trajectory based on the surface wind field was obtained using MC2 and other software that was constrained to pass over the urban core of Vancouver at 8:00 during the morning rush hour. The trajectory started at 6:00 a.m. over the ocean about 15 km west of the coast. After

Table 1. Emitted VOC model species

Model Species	Description
CH ₄	Methane
ETHE	Ethene
MEOH	Methanol
ETOH	Ethanol
MTBE	Methyl <i>t</i> -butyl ether
HCHO	Formaldehyde
CCHO	Acetaldehyde
RCHO	Propionaldehyde and higher aldehydes
MEK	Methyl ethyl ketone and higher ketones
CRES	Cresols and other alkyl phenols
MGLY	Methyl glyoxal
ALK1	First lumped group for alkanes whose OH rate constants are $< 1.0\text{E}4 \text{ ppm}^{-1} \text{ min}^{-1}$
ALK2	Second lumped group for alkanes whose OH rate constants are $> 1.0\text{E}4 \text{ ppm}^{-1} \text{ min}^{-1}$
ARO1	First lumped group for aromatics whose OH rate constants are $< 2.0\text{E}4 \text{ ppm}^{-1} \text{ min}^{-1}$
ARO2	Second lumped group for aromatics whose OH rate constants are $> 2.0\text{E}4 \text{ ppm}^{-1} \text{ min}^{-1}$
OLE1	First lumped group for anthropogenic alkenes whose OH rate constants are $< 7.5\text{E}4 \text{ ppm}^{-1} \text{ min}^{-1}$
OLE2	Second lumped group for anthropogenic alkenes whose OH rate constants are $> 7.5\text{E}4 \text{ ppm}^{-1} \text{ min}^{-1}$
OLE3	Third lumped group for primarily biogenic alkenes (isoprene, terpenes)

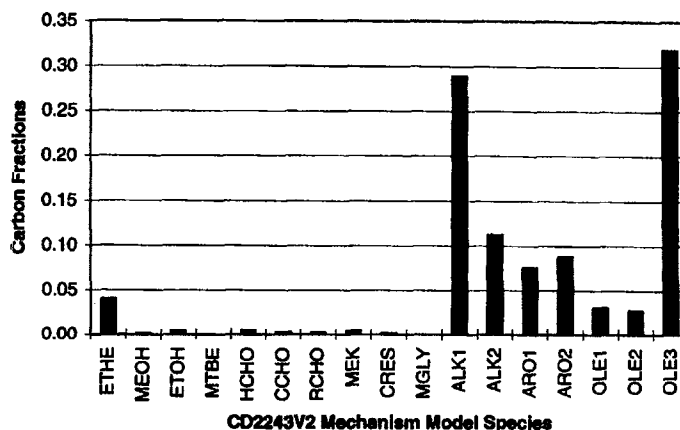


Fig. 2. LFV non-methane-organic compound (NMOC) emissions profile represented as the model species in the CD2243V2 mechanism.

Table 2. Comparison of carbon numbers and rate constants for the COND2243 and CD2243V2 mechanisms

VOC model species	# of C's		Δ	$\Delta\%$
	COND2243	CD2243V2		
ALK1	4.50	4.62	0.12	2.67
ALK2	7.53	7.53	0.00	0.00
ARO1	7.13	7.22	0.09	1.26
ARO2	8.56	8.69	0.13	1.52
OLE1	3.79	3.86	0.07	1.85
OLE2	4.76	4.91	0.15	3.15
OLE3	6.53	8.55	2.02	30.93

Reactions	k ($\text{cm}^3 \text{molec}^{-1} \text{s}^{-1}$)		Δ	$\Delta\%$
	COND2243	CD2243V2		
ALK1 + OH	3.712E-12	3.597E-12	- 1.150E-13	- 3.10
ALK2 + OH	1.049E-11	1.297E-11	2.482E-12	23.67
ARO1 + OH	5.869E-12	5.869E-12	0.000E + 00	0.00
ARO2 + OH	2.980E-11	2.728E-11	- 2.521E-12	- 8.46
OLE1 + OH	2.993E-11	3.183E-11	1.897E-12	6.34
OLE1 + O ₃	1.176E-17	1.183E-17	6.400E-20	0.54
OLE1 + O	4.903E-12	5.862E-12	9.594E-13	19.57
OLE1 + NO ₃	3.396E-14	6.022E-14	2.627E-14	77.36
OLE2 + OH	6.392E-11	6.556E-11	1.643E-12	2.57
OLE2 + O ₃	1.785E-16	2.025E-16	2.403E-17	13.46
OLE2 + O	2.376E-11	2.514E-11	1.378E-12	5.80
OLE2 + NO ₃	1.054E-12	1.312E-12	2.575E-13	24.43
OLE3 + OH	1.026E-10	7.091E-11	- 3.168E-11	- 30.88
OLE3 + O ₃	3.422E-17	5.248E-17	1.827E-17	53.38
OLE3 + O	5.062E-11	3.839E-11	- 1.223E-11	- 24.16
OLE3 + NO ₃	2.089E-12	3.663E-12	1.573E-12	75.29

passing over Vancouver, it continues in a generally easterly direction, travelling over forested areas at the end of the day. The trajectory is shown in Fig. 1.

The horizontal dimensions of the air mass were taken as $20 \times 20 \text{ km}^2$. The hourly emissions into the air mass were taken from the $5 \times 5 \text{ km}^2$ gridded emissions inventory, with the emissions from each grid weighted by the extent of coverage by the air mass. The hourly mixing height, temperature, and humidity, shown in Table 3, were taken from the corresponding grids of the MC2 simulation. For the last two hours of the simulation, the air mass had moved outside the boundary of the anthropogenic emissions inventory into a predominantly forested region. For these two hours, the emissions were estimated based on the geographical features of the region, where there were only biogenic emissions.

Since the air mass started over the ocean in the early morning, it is assumed that the air mass was very clean. The assumed initial ground-level concentrations were: O₃ 15 ppb; VOC 10 ppbC; NO_x 1 ppb; CO 200 ppb. The initial aloft concentrations were: O₃ 20 ppb; VOC 20 ppbC; NO_x 2 ppb; CO 200 ppb. These values are consistent with the typical observed concentration ranges for regions between remote marine sites and urban sites (NRC, 1991; Chameides *et al.*, 1992). The NO_x and VOC concentrations were interpolated values between the remote marine sites and the urban sites. The O₃ concentration is set at the lower end of the marine site O₃ range. The selected ground-level VOC concentration of 10 ppbC also matches with the recommendation by Moore *et al.* (1991). The CO concentration of 200 ppb is the typical value for remote areas (Finlayson-Pitts and Pitts, 1986). The initial CH₄ concentration is set to the global background value of 1.79 ppm. Speciation of the initial VOC is based on the average VOC emissions in our modelling domain as shown in Fig. 2. Since the initial air mass is clean, any difference in model results caused by various speciation of initial VOC is very small.

Table 3. Mixing height, temperature and relative humidity along the trajectory

Hour	M.H. (m)	T (K)	R.H. (%)
6:00	100.0	291	72
7:00	98.9	292	73
8:00	457.9	294	71
9:00	440.4	295	70
10:00	448.7	297	68
11:00	470.9	298	66
12:00	542.2	299	38
13:00	617.7	299	37
14:00	669.8	299	34
15:00	697.1	299	32
16:00	709.2	299	27
17:00	735.8	300	28
18:00	616.1	299	28
19:00	564.8	298	32
20:00	513.4	297	36
21:00	462.2	296	40
22:00	410.7	295	44

3. SENSITIVITY OF OZONE CONCENTRATIONS TO VOC AND NO_x EMISSIONS

3.1. The contribution of base case emissions to ozone levels

Hourly speciated base case emissions along the air mass trajectory are given in Fig. 3. Units of "moles" and "moles C" are used for NO_x emissions (NO and

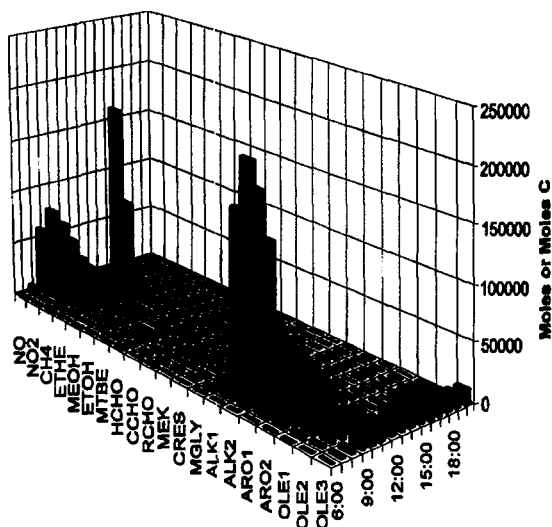


Fig. 3. Hourly emissions entered into the moving air mass. The emissions are speciated in the CD2243V2 mechanism model species. Units for the emitted NO_x and VOC model species are "moles" and "moles C", respectively.

NO_2) and VOC emissions, respectively. In the early morning hours of 6:00 to 7:00, the amount of emissions was very small as the air mass travelled mostly over the ocean. From 8:00 a.m. to 2:00 p.m., the emissions were high as the air mass passed through the urban core. The emissions came from various sources including both anthropogenic and biogenic sources during the period. However, the main sources were anthropogenic, with major emissions identified by the species NO , ALK1 , ALK2 , ARO1 , ARO2 , OLE1 , OLE2 , ETHE and CH_4 in the mechanism. At around 2:00 p.m., the air mass moved into a mountainous area. The total emissions dropped substantially and the emissions mostly came from biogenic sources. The biogenic emissions are shown as OLE3 . For the whole simulation period, the average VOC/ NO_x ratio of the emissions is 7.7.

To see the contribution of base case emissions to the ozone levels, both VOC and NO_x are set to zero in the first test. Without the VOC and NO_x emissions, the whole system is driven by chemistry and meteorology operating on the initial concentrations. As shown in Fig. 4, the peak ozone concentration is 44.9 ppb in this situation. When base case VOC and NO_x emissions are added to the system, the ozone levels first decrease in the early hours due to the titration of ozone by NO . The ozone levels then increase until late afternoon, reaching a peak value of 66.3 ppb. The contribution of the base case emissions to the peak ozone is thus 21.4 ppb.

3.2. Sensitivity of O_3 concentrations to the total VOC and total NO_x emissions

Selected sensitivity tests of O_3 concentrations to the total VOC emissions are shown in Fig. 5. VOC emissions are multiplied by 0, 0.8, ..., 2 and NO_x emis-

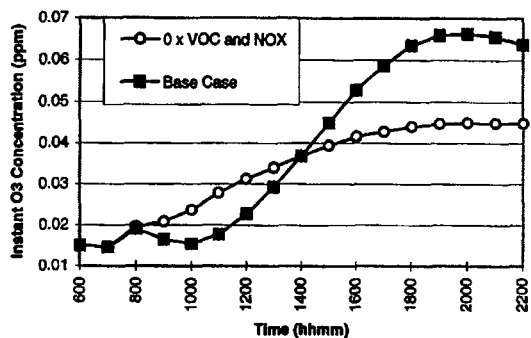


Fig. 4. Contribution of total base case VOC and NO_x emissions to ozone levels. "0 x VOC and NO_x " stand for zero VOC and NO_x emissions; "Base case" stands for the base case VOC and NO_x emissions.

sion is kept at the base case amount. Instantaneous O_3 concentration curves are plotted along with a curve which is produced by the zero VOC and NO_x emissions case. The curve corresponding to zero VOC and NO_x emissions will be referred to as the zero emission curve. The history of base case NO_x and VOC emissions into the moving air mass is also shown at the bottom of Fig. 5.

In general, the O_3 concentrations increase with increasing VOC emissions. However, between 8:00 and 9:00 in the morning, all air masses have negative reactivities in terms of O_3 production even in the case that VOC emissions are doubled. This can be explained by the NO_x predominance in this hour. O_3 titration by NO is the predominant chemical process at this time. In fact, the O_3 destruction by NO is so strong in the morning that it is not totally offset by the O_3 production process until about 10:40 a.m. even if VOC emissions are doubled. This is evidenced by the crossing of the $2 \times$ VOC curve with the zero emission curve at about 10:40 a.m. For the base case VOC emissions, the crossing does not appear until 14:00 in the afternoon. For a VOC emission reduction of 20% (see $0.8 \times$ VOC curve), the crossing occurs at 16:25. For a VOC emission reduction of more than 25%, crossing of the zero emission curve and the VOC reduction curve does not happen at all. In this case, the net effect of all VOC and NO_x emissions along the air mass trajectory is O_3 destruction instead of O_3 production.

Sensitivity of peak O_3 concentrations to the total VOC emissions depends on the total amount of emitted VOC. The sensitivity is close to a maximum when our base case VOC emissions are multiplied by 1.2. Generally speaking, increasing VOC emissions will increase the O_3 levels and decreasing the emissions will have an opposite effect. However, the effect becomes smaller when the amount of emissions is moved away from the $1.2 \times$ VOC case.

Figure 6 presents the O_3 sensitivity to the total amount of NO_x . In these tests, NO_x emissions are multiplied by different factors ranging from 0 to 2.0,

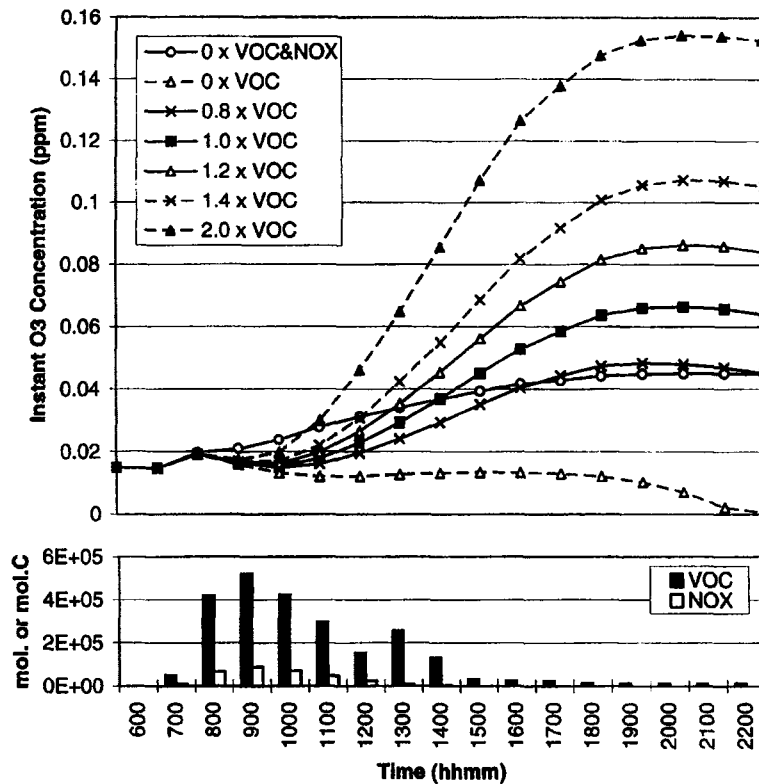


Fig. 5. Sensitivity of O₃ concentrations to total VOC emissions. Legend examples: 0.8 x VOC: Base case VOC emissions are multiplied by 0.8. 0 x VOC&NOX: Both VOC and NO_x emissions are zero. The history of base case NO_x and VOC emissions into the moving air mass is shown at the bottom part. The units "mol" and "mol C" are used for the emissions of NO_x and VOC, respectively.

while VOC emissions are fixed at the base case amount. Since the change of O₃ concentrations with NO_x emissions is not monotonic, the plots in Fig. 6a have many crossings among the curves. Figure 6b gives a better three-dimensional view of Fig. 6a. Similar to the figure for the VOC emissions sensitivity test (Fig. 5), a curve with zero VOC and NO_x emissions is also plotted in Fig. 6.

The highest O₃ level occurs when NO_x emissions are reduced by about 60%. This corresponds to the 0.4 x NO_x curve in Fig. 6. When the NO_x emissions are at this level, total net O₃ production efficiency is the highest. When NO_x emissions are lower than this level, the O₃ titration is weaker and the O₃ concentrations are higher in early morning hours. However, later in the day, O₃ concentrations for the 0.4 x NO_x emission case quickly catch up and pass the levels obtained by the lower NO_x cases. They overtake the 0.2 x NO_x case at about 13:40 and overtake the zero NO_x emission case at 11:00. When NO_x emissions are higher than 0.4 times the base case emissions, the peak O₃ concentrations are always lower than those achieved by 0.4 times the base case emissions. The higher the NO_x emissions, the lower the O₃ concentrations are in these cases. As long as the emissions are higher than 1.17 times the base case NO_x emissions, O₃ concentrations are always lower than the case of

zero NO_x emissions. When the NO_x emissions are higher than 1.3 times the base case NO_x emissions, O₃ concentrations are even lower than the case that there is no NO_x and VOC emissions at all.

Therefore, VOC control is the key to achieve lower O₃ levels when total NO_x emissions are 0.4 times our base case NO_x emissions or higher. Control of NO_x emissions in order to control O₃ levels will be counterproductive under the conditions for our base case simulations. When the NO_x emissions are lower than 0.4 times of the base case NO_x emissions, NO_x control will be effective in controlling maximum O₃ at downwind locations in the afternoon or early evening. However, the control will boost morning O₃ levels in the urban areas.

3.3. Sensitivity of O₃ concentrations to emissions of individual model species

When emissions of individual model species are changed by a certain factor, the response of O₃ concentrations to the change is variable. The sensitivity of O₃ concentrations depends on the O₃-producing or O₃-titrating capability and the amount of emissions of the model species.

3.3.1. Sensitivity of O₃ concentrations to emissions of individual VOC model species. The emitted VOC model species in the LFV can be classified into three

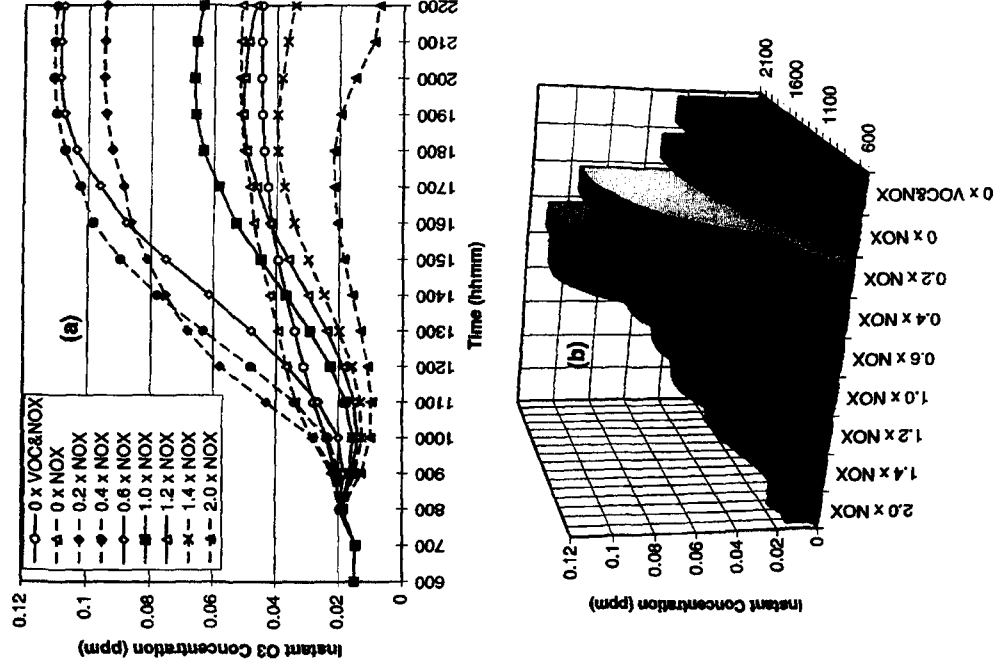


Fig. 6. Sensitivity of O₃ concentrations to total NO_x emissions. (a) a two dimensional plot; (b) a three dimensional plot. Legend is the same as in Fig. 5 except that NO_x is used instead of VOC.

categories according to the contribution of their emissions to the base case maximum 1 h average ozone concentration and according to the sensitivity of the ozone concentration to a fractional change of the emissions. Table 4 lists the species in the three categories.

In Table 4, the "model species contribution" to the base case ozone concentration is shown in two columns. The first column lists the differences between the base case ozone concentration and those achieved by setting emissions of individual model species to zero, one at a time. For example, the maximum 1 h average ozone concentration is 66.3 ppb when base case emissions of all species are used. If the ARO2 emissions are set to zero, the maximum ozone concentration becomes 38.81 ppb. This suggests that the ARO2 emissions in the base case contribute 27.49 ppb to the base case maximum ozone concentration. In relative terms, the base case ARO2 emissions contribute 41.48% of the base case maximum ozone. The relative contributions are shown in the column under "%" in Table 4.

The average sensitivities in Table 4 are expressed in two ways and also listed in two columns. The basic definition for the average sensitivity is

$$\text{Average sensitivity} = \frac{\Delta(\text{max. O}_3)}{\Delta\text{VOC}(i)} \times 100 \quad (1)$$

where VOC(*i*) is the base case amount of emissions of the *i*th emitted VOC species. ΔVOC(*i*)/VOC(*i*) is chosen to be

$$\frac{\Delta\text{VOC}(i)}{\text{VOC}(i)} = \frac{1.2 \times \text{VOC}(i) - 0.8 \times \text{VOC}(i)}{\text{VOC}(i)} = 0.4.$$

Therefore, the calculated average sensitivity is for the emissions range 0.8 × VOC(*i*) to 1.2 × VOC(*i*). Note that the average sensitivity based on equation (1) has a unit ppb O₃/%emi, which shows change in maximum 1 h average O₃ in ppb for each percentage change in the emissions. The average sensitivity proposed here is different from the reactivity scales defined by Carter (1994) and other authors. The average

Table 4. Sensitivity of maximum 1 h average ozone concentration to emissions of VOC model species in the LFV

Category	Model species VOC(i)	Model species contribution ^a		Average sensitivity ^b	
		ppb	%	ppbO ₃ /%emi.	%O ₃ /%emi.
Significant	ARO2	27.49	41.48	0.31	0.47
	OLE2	11.89	17.94	0.12	0.18
	ETHE	10.22	15.42	0.11	0.17
	OLE1	9.49	14.32	0.09	0.14
	ALK1	8.81	13.29	0.08	0.12
	OLE3	8.02	12.10	0.09	0.13
	ARO1	6.39	9.64	0.06	0.09
	ALK2	5.84	8.81	0.06	0.08
	HCHO	2.83	4.27	0.02	0.04
Mod.-influential	RCHO	0.68	1.03	0.01	0.01
	CCHO	0.61	0.92	0.01	0.01
Non-influential	MEK	0.22	0.33	0.00	0.00
	CRES	0.15	0.23	0.01	0.01
	MGLY	0.10	0.15	0.00	0.00
	MTBE	0.07	0.11	0.00	0.00
	MEOH	0.06	0.09	0.00	0.01
	ETOH	0.03	0.05	0.00	0.00
	CH ₄	0.01	0.02	0.00	0.00

^a A model species contribution to ozone is calculated as the difference in ozone between the base case (66.3 ppb) and a simulation in which the emissions of the species is set to zero.

^b The average sensitivities are calculated for the range of $0.8 \times \text{VOC}(i)$ to $1.2 \times \text{VOC}(i)$ emissions.

sensitivity here is directly related to the real amount of base case emissions and reflects the emissions characteristics of a specific region. For some emitted VOC species such as methyl glyoxal (MGLY), the specific reactivity values are very high but the amount emitted in the LFV is very small. Therefore, their average sensitivities are very low and no significant reduction in O₃ can be achieved by controlling the emissions of these species in the LFV. The opposite situation exists for some other species such as the slowly reacting alkane group ALK1, which has low specific reactivity but has a high emission rate.

In Table 4, the average sensitivities are also shown in percentage changes in maximum 1 h average O₃ for each percentage change in the *i*th VOC species emissions (% O₃/% emi.). The numbers reflect relative changes in the maximum O₃ concentrations due to a percentage change of emissions.

3.3.1.1. Significant species. These are the species whose emissions have significant impact on the O₃ levels in the LFV. Base case emissions of each of the species contribute more than 4% to the base case maximum 1 h average ozone level, i.e. the O₃ level would be at least 4% lower without emissions of any one of the species. The O₃ concentrations are also sensitive to the emissions change close to the base case amount of emissions of the species. The average O₃ sensitivity in the range of $0.8 \times \text{VOC}(i)$ to $1.2 \times \text{VOC}(i)$ emissions is 0.04% increase of O₃ per percent increase of the model species emissions or higher. In terms of ppb O₃, the sensitivity is at least 0.02 ppb O₃ per % emissions change.

This category includes 9 VOC model species. Some of the species in this category, e.g. ETHE, are highly

reactive. Reduction of a moderate amount of their emissions can have an observable effect. However, reactivities of some of the species, such as ALK1, are moderate on a per carbon basis. Their significant impacts on ozone concentrations in the LFV are caused by their relatively high emissions.

Among the 9 model species in this category, the most significant species is ARO2. Both its reactivity and amount of emissions are high. Combination of the two effects makes ARO2 the most significant species in terms of both its total contribution to the O₃ concentrations and the sensitivity of O₃ concentrations to small percentage changes in emissions. Figure 7 shows the O₃ concentrations for different emission rates of ARO2. The base case emissions are multiplied by 0, 0.2, ..., 2.0, respectively. The wide gap between the 0 × emissions curve (0 × ARO2) and the 1.0 × emissions curve (1.0 × ARO2) shows the significant contribution of the base case ARO2 emissions to the O₃ concentrations. Wide spacings between the 0.8 × emissions and 1.0 × emissions curves as well as the 1.0 × emissions and 1.2 × emissions curves reveal the large O₃ sensitivity. From Table 4, we can see that the maximum O₃ concentration can be reduced by 41.48% by eliminating ARO2 emissions alone. According to Figure 7, the maximum O₃ concentration increases about 50% if ARO2 emissions are doubled. For every percent increase of ARO2 emissions close to the base case amount, maximum 1 h average O₃ increases approximately 0.47% or 0.31 ppb.

One unique feature for ARO2 is that controlling ARO2 alone can achieve the same or better results than controlling all VOC and NO_x emissions. For comparison purposes, an O₃ curve corresponding to

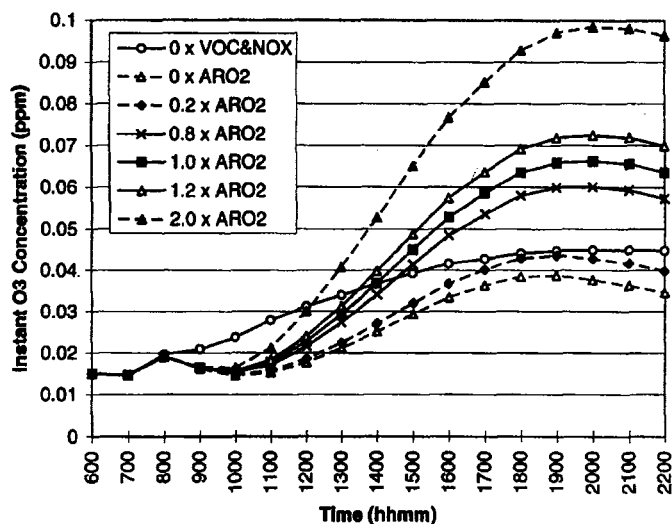


Fig. 7. Sensitivity of O_3 concentrations to ARO2 emissions in the LFV. Legend is the same as in Fig. 5 except that ARO2 instead of VOC is used.

zero emissions is plotted in Fig. 7. According to the figure, if ARO2 emissions are cut 75% or more, the O_3 concentrations will always be lower than the O_3 concentrations corresponding to zero emissions at any time. It should be noted that the results presented here are based on the chosen trajectory under the specific conditions. The results show that ARO2 is the most significant model species based on the impact of its emissions on O_3 concentrations. Quantitative application of the results to other situations should be done cautiously.

3.3.1.2. Moderately influential species. Emission changes of the model species in this category have moderate impact on O_3 concentrations. Acetaldehyde (CCHO) and higher aldehydes (RCHO) belong to this category. They have both rather strong O_3 -producing reactivities and non-negligible amounts of emissions in the LFV. According to Table 4, the base case emissions of CCHO and RCHO contribute about 0.92% (0.61 ppb) and 1.03% (0.68 ppb) to the peak O_3 levels, respectively. The average sensitivities for CCHO and RCHO are both 0.01% O_3 per percentage change in emissions.

Figures that show O_3 concentration curves for changed amounts of emissions of CCHO and RCHO are not presented here for simplicity. The plots are similar to those in Fig. 7 except that the curves are much closer to each other for moderately influential species. The differences in O_3 concentrations among the curves are noticeable, spanning a range of about 2 ppb in the afternoon.

3.3.1.3. Non-influential species. O_3 concentration changes caused by change in emission of these species are hardly noticeable when the emissions are multiplied by a factor of 0–2.0. The highest contribution of base case emissions in this category to the maximum O_3 concentration is 0.22 ppb or 0.33%. The highest average sensitivity is about 0.01 ppb O_3 per percent-

age change in emissions. Both the base case emission contribution and the sensitivity are negligible.

A representative in this category is methyl glyoxal (MGLY), which has been mentioned at the beginning of this section. Although the results are not shown here, all 11 curves generated by the base case MGLY emissions multiplied by 0, 0.2, ..., 2.0 overlap each other, if plotted analogously to Fig. 7. The insensitivity is caused by the very low amount of MGLY. Note that our discussion here is based on the amount of emissions in the LFV. If MGLY emissions were equal to the amount of emissions of other model species, calculations show that the reactivity of MGLY would be very high. In contrast to MGLY, methane, another typical species in this category, has a very high level of emissions. The insensitivity of ozone yield to the change of methane emissions is caused by the low reactivity of methane itself.

Including MGLY and methane, the category of non-influential species in the LFV consists of 7 emitted VOC model species, which are listed in Table 4. Among them, CH_4 , the main component in natural gas, is a candidate for evaluation as an alternative fuel. MEOH and ETOH can be used as alternative fuels or additives to make reformulated gasolines. MTBE is used as an additive in some reformulated gasolines.

Note that the above classification of VOC model species is somewhat arbitrary in terms of selecting the quantitative criteria for the classification. The classification provides a guide in determining the relative importance of emissions in model species in the LFV. This information is important in evaluating emissions control strategies and in analysing the emissions inventory.

3.3.2. Sensitivity of O_3 concentrations to NO and NO_2 emissions. Response of O_3 concentrations to changed NO and NO_2 emissions are qualitatively different. Figure 8 shows the results of changing the

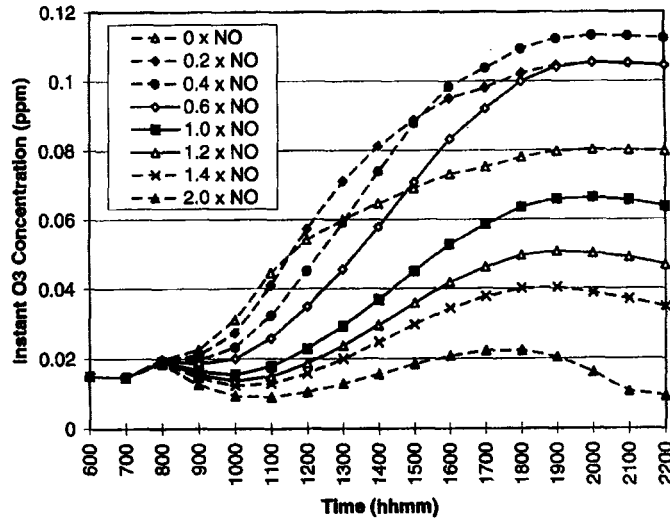


Fig. 8. Sensitivity of O_3 concentrations to NO emissions. Legend is the same as in Fig. 5 except that NO instead of VOC is used.

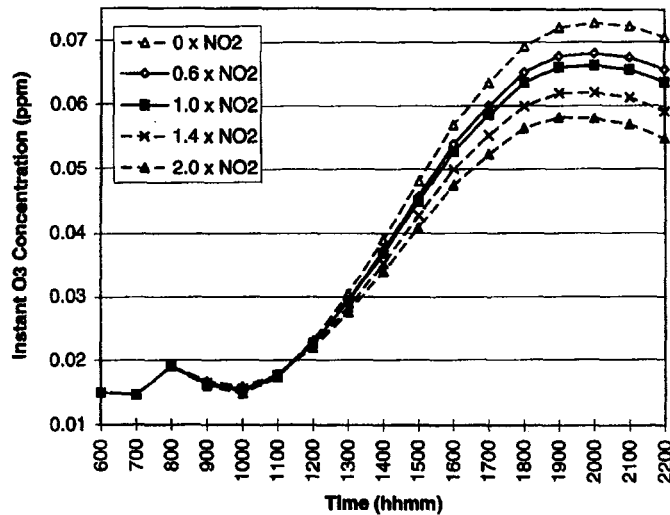


Fig. 9. Sensitivity of O_3 concentrations to NO_2 emissions. Legend is the same as in Fig. 5 except that NO_2 instead of VOC is used.

base case NO emissions while keeping NO_2 emissions at the base case level. Figure 9 shows the results of changing NO_2 emissions while fixing NO emissions.

NO makes up 90% of the LFV NO_x emissions, with the remainder NO_2 . Therefore, it is anticipated that the response of O_3 concentrations to changed NO emissions is similar to the response of O_3 to changed total NO_x emissions. Comparing Fig. 8 with Fig. 6(a), we can see the similarity. Maximum O_3 concentrations achieved by 0.4 times of base case emissions are 113 and 111 ppb in Fig. 8 and Fig. 6(a), respectively. However, the peak O_3 corresponding to 0 x NO and 0.2 x NO emissions in Fig. 8 are 80 and 105 ppb, respectively. They are much higher than the peak O_3 concentrations achieved by 0 x NO_x and 0.2 x NO_x emissions, which are 52 and 95 ppb, in

Fig. 6(a). The explanation is based on NO_2/NO_x ratios. In Fig. 6(a), we multiply total NO_x emissions by a factor without changing emitted NO_2/NO_x ratios. In Fig. 8, only NO emissions are lowered by a multiplication factor. This lowers total NO_x emissions and increases the NO_2/NO_x ratios. Both of these changes benefit net O_3 production. Therefore, the increases in O_3 concentrations are more dramatic in Fig. 8 than in Fig. 6(a).

In contrast to what may be expected, O_3 concentrations get a boost from decreased NO_2 emissions. According to Fig. 9, completely eliminating NO_2 would increase peak O_3 by 6.6 ppb, which is 10.0% of the base case peak O_3 concentration of 66.3 ppb. Doubling NO_2 would decrease peak O_3 by 8.1 ppb. The net effect of increased NO_2 emissions will depend

In this paper, sensitivities of O_3 concentrations to both total and speciated NO_x and VOC emissions models

4. DISCUSSION AND CONCLUSIONS

It was found that both NO and NO_2 have negative impacts on O_3 concentrations in the urban plume in the LTV over a one day period. Any overestimation of NO_x emissions in the emissions inventory could cause underprediction of ozone levels by photochemical models

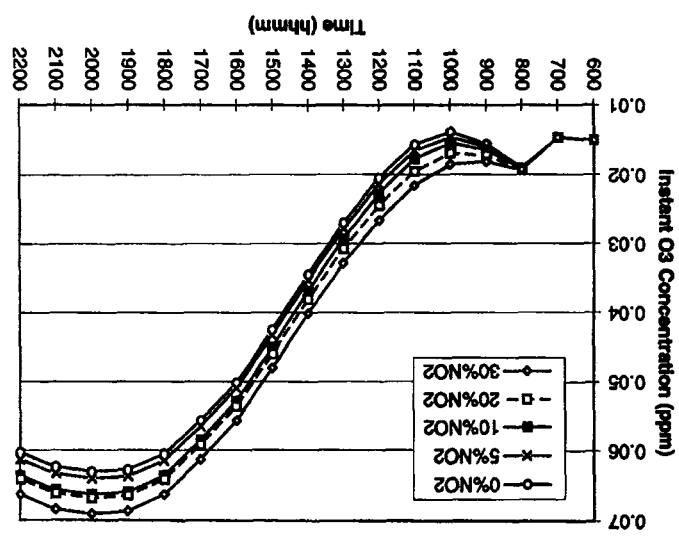
ozone formation. gasoline fuels could have a significant impact on line sold in the valley. Control of aromatics content in is largely determined from the composition of gaso- In turn, the quantity of aromatics from these sources and evaporative emissions from the LDGV (10.2%), vehicles (LDGV) (54.3%), gasoline marketing (22.2%) are exhaust emissions from light-duty gasoline. The major sources of ARO_2 in the emissions inven- contains mostly isomers of xylene (41.5%), trimethyl- urban plume. In the LTV emissions inventory, ARO_2 alone would achieve significant O_3 reductions in the studies indicate that reducing emissions of ARO_2 important emitted VOC model species. The sensitivity ing reactive aromatics, was found to be the most- tations in the LTV. Among them, ARO_2 , represent- based on the impact of their emissions on O_3 concen- Nine significant VOC model species were identified

egies. valuable for development of emission control strat- on emissions characteristics in the region and is species. In this approach, the sensitivity depends tivity and emitted amounts of each VOC model tivity used in this paper depends on both the reac- each emitted VOC model species. The average sensi- and average O_3 sensitivities are calculated for 1985. Both contributions of base case emissions urban core of Vancouver, for a specific period in July and of scavenging of radicals like OH by NO_2 (to on the relative rates of NO_2 photolysis (to form O_3)

emissions and that the latter process is more impor- Another uncertain factor related to the NO_x emis- sions is the NO_2/NO_x ratio. Although it is very well understood that the majority of NO_x in emissions inventories is NO , the quantitative ratio of NO_2/NO_x or NO/NO_x is not a well-determined factor. The de- fault NO_2/NO_x ratio in Emissions Preprocessor Sys- tem 2.0 (EPS2) is 10% while it is 5% in OZIPR modelling software. Figure 10 shows the response of O_3 concentrations to changed NO_2/NO_x ratios when the total amount of NO_x emissions is fixed. As ex- pected, higher NO_2/NO_x ratios cause higher O_3 con- centrations. This is because a higher NO_2/NO_x ratio means relatively higher O_3 -production potential and lower O_3 -titration rate. The effect of lower O_3 -titra- tion rate can be seen clearly from Fig. 10. Comparing Fig. 10 with Figs 5-9, we can see that the curves in Fig. 10 are more parallel to each other after 10:00 a.m.

This is caused by significant decrease in O_3 -titration rates in early morning hours when NO_2/NO_x ratios are increased, while the changes in O_3 -production rates later in the day are relatively insignificant. Vary- ing the NO_2/NO_x ratios from 0 to 30% results in peak O_3 concentrations of 63.0-69.0 ppb. The change is equivalent to 9.0% of the base case amount of peak ozone.

Fig. 10. Sensitivity of O_3 concentrations to NO_2/NO_x ratios in emissions. Total NO_x emissions are fixed at the base case amount while the NO_2/NO_x ratio (in %) is varied.



In usual applications of trajectory models, the trajectory is selected based on the final destination of an air mass. The destination is selected to coincide with the location of a monitoring station so that final calculated concentrations can be compared with observations. In the present work, the trajectory was selected to track an air mass that passed over the urban core during the morning rush hour so that the sensitivity to emissions can be studied. Similar to other modelling studies using three-dimensional models, calculated maximum ozone concentrations in this paper using base case emissions are substantially lower than the maximum ambient ozone concentrations, which is more than 100 ppb during the episode. Better agreement with observed ozone concentrations could be obtained by adjustments to the emissions according to the sensitivity tests discussed in this paper. However, the adjustment can only be done after carefully evaluating other uncertainties in the modelling process, and any adjustments have to be validated using three-dimensional models.

The sensitivity of ozone concentrations to both the total and the speciated emissions reported here can be used to identify portions of the LFV emissions inventory that require further scrutiny. Based on the results in this paper, particular attention will be paid to the mass and speciation profiles of gasoline vehicle exhaust and evaporative emissions, which are major contributors to NO_x and ARO₂ emissions. Studies have been initiated to examine VOC speciation profiles for the SCC codes related to the gasoline vehicle emissions and to compare them with profiles derived from a tunnel study in the LFV. A detailed comparison of VOC compositions in the emissions inventory and ambient data has also been conducted and will be published elsewhere. These studies necessarily include consideration of historical gasoline RVP values in the LFV over the past decade and their impact on VOC speciation.

Acknowledgements—The authors would like to thank Dr William P. L. Carter at University of California, Riverside, Dr Fred Lurmann and Dr Naresh Kumar at STI for their timely help in implementing Carter's mechanism preparation package. Special thanks are also extended to Dr Neil Wheeler, Dr Donald Johnson and Bart Croes at the California Air Resources Board for their software and documentation support. Ms Susan Bohme and Mr Alfred Dorkalam helped process the emissions inventory and provided technical assistance to the project. Their contribution is deeply appreciated.

This project is supported by Natural Resources Canada and the National Research Council of Canada.

REFERENCES

- Carter W. P. L. (1988) Documentation for the SAPRC atmospheric photochemical mechanism preparation and emissions processing programs for implementation in airshed models. Prepared for the California Air Resources Board Contract No. A5-122-32. Statewide Air Pollution Research Center, University of California, Riverside, California.
- Carter W. P. L. (1990) A detailed mechanism for the gas-phase atmospheric reactions of organic compounds. *Atmospheric Environment* **24A**, 481–518.
- Carter W. P. L. (1994) Development of ozone reactivity scales for volatile organic compounds. *J. Air Waste Man. Ass.* **44**, 881–899.
- CCME (1990) Management plan for nitrogen oxides (NO_x) and volatile organic compounds (VOCs) phase I. Canadian Council of Ministers of the Environment.
- Chameides W. L., Fehsenfeld F., Rodgers M. O., Cardelino C., Martinez J., Parrish D., Lonneman W., Lawson D. R., Rasmussen R. A., Zimmerman P., Greenberg J., Middleton P. and Wang T. (1992) Ozone precursor relationships in the ambient atmosphere. *J. geophys. Res.* **97**, 6037–6055.
- Finlayson-Pitts B. J. and Pitts J. N. Jr (1986) *Atmospheric Chemistry: Fundamentals and Experimental Techniques*. Wiley, New York.
- Gardner L., Causley M., Wilson G. and Jimenez M. (1992) User's guide for the urban airshed model, Vol. IV. *User's Manual for the Emissions Preprocessor System 2.0*. U.S. Environmental Protection Agency, Research Triangle Park, North Carolina.
- Gery M. W. and Crouse R. R. (1989) *User's Guide for Executing OZIPR*. Atmospheric Research and Exposure Assessment Laboratory, U.S. Environmental Protection Agency, Research Triangle Park, North Carolina.
- Hogo H. and Gery M. W. (1988) *Users Guide for Executing OZIPM-4 with CBM-IV or Optional Mechanisms*. Vol. 1. *Description of the Ozone Isopleth Plotting Package-Version 4*. U.S. Environmental Protection Agency, Research Triangle Park, North Carolina.
- McLaren R., Bohme S., Hedley M., Jiang W., Dorkalam A. and Singleton D.L. (1995) Emissions inventory processing for UAM-V and CALGRID modelling in the lower Fraser Valley. *Proc. Int. Symp. The Emissions Inventory: Programs and Progress*, Research Triangle Park, North Carolina, Air & Waste Management Association, October, 1995.
- Moore G. E., Killus J. P. and Whitten G. Z. (1991) Composition of marine air offshore of the western United States. *J. appl. Met.* **30**, 707–713.
- NRC (National Research Council) (1991) Rethinking the ozone problem in urban and regional air pollution. National Academy Press, Washington, District of Columbia.
- Tanguay M., Robert A. and Laprise R. (1990) A semi-implicit semi-Lagrangian fully compressible regional forecast model. *Mon. Weath. Rev.* **118**, 1970–1980.
- Yamartino R. J., Scire J. S., Carmichael G. R., and Chang Y. S. (1992) The CALGRID mesoscale photochemical grid model—I. Model formulation. *Atmospheric Environment* **26A**, 1493–1512.
- Yang Y., Stockwell W. R. and Milford J. B. (1995) Uncertainties in incremental reactivities of volatile organic compounds. *Envir. Sci. Technol.* **29**, 1336–1345.